



Velocity profile report at the seismic station IT.SNZ1 - San Nazzaro (PC)

Report sul profilo di velocità sismica per il sito della stazione sismica IT.SNZ1 - San Nazzaro (PC)

Working Group: Claudia MASCANDOLA Sara LOVATI Marco MASSA	Date: Dicembre 2019
Subject: Final report illustrating measurements, analysis and results for Vs profile at station IT.SNZ1	



INDEX

1. Introduction	3
2. Geophysical Investigations	4
3. Seismic Velocity Model	13
4. Conclusions	19
<i>References</i>	21
<i>Disclaimer and limits of use of information</i>	22
<i>Esclusione di responsabilità e limiti di uso delle informazioni</i>	23



1. INTRODUCTION

In this report, we present the geophysical measurements and the results obtained in the framework of the 2019-2021 agreement between INGV and DPC, Allegato B2, WP1 - TASK 2: "Caratterizzazione siti accelerometrici" (Coord.: G. Cultrera, F. Pacor). In this report, the results for station IT.SNZ1, belonging to the Italian Strong Motion Network (RAN-DPC), are presented. The recording station is located in the Po Plain area, specifically in the town of San Nazzaro that belongs to the municipality of Monticelli d'Ongina, in the province of Piacenza.

Geophysical measurements consist in ambient-vibration measurements in both single-station and 2D array configuration that provide results in terms of resonance frequency of the soil deposits and in terms of dispersion curves of surface waves. These curves are inverted to obtain a shear-wave velocity (V_s) profile that is suitable for assigning the soil class according to the current Italian seismic code (NTC 2018) and the current Eurocode (EC8).



2. GEOPHYSICAL INVESTIGATIONS

Figure 1 shows the location of the IT.SNZ1 seismic station (in red) and the location of the seismic stations used for the 2D array (in yellow). The distance between IT.SNZ1 seismic station and the center of the 2D array (NAZ5) is 173 m. The seismic sensors were positioned in a circular geometry, with a radius of 50 m, in order to have a homogeneous azimuthal coverage that allows a better performance of the array techniques. The corresponding geographic coordinates are reported in Table 1.

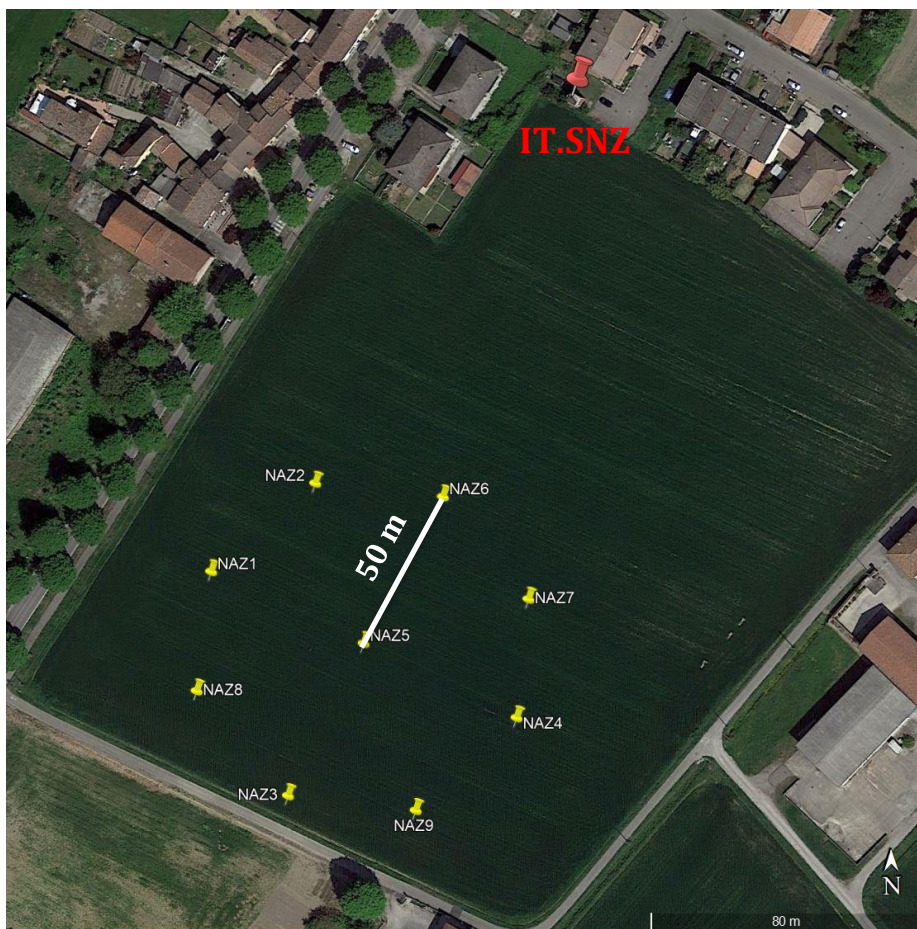


Figure 1: Map of the geophysical measurements performed at the IT.SNZ1 site. The yellow points are the nine stations of the 2D array in passive configuration. The red point indicates the IT.SNZ1 seismic station.



Station	Lat. [°]	Lon. [°]	El. [m]
NAZ1	45.073000	9.893107	34
NAZ2	45.073230	9.893500	38
NAZ3	45.072405	9.893383	33
NAZ4	45.072603	9.894242	34
NAZ5	45.072805	9.893673	34
NAZ6	45.073190	9.893977	35
NAZ7	45.072917	9.894292	34
NAZ8	45.072685	9.893047	33
NAZ9	45.072362	9.893860	39

Table 1: geographic coordinates of the array stations (WGS84).

All stations of the array are equipped with Reftek-130 digitizer and Lennartz 3D-5s velocimetric sensors. The measurements were recorded in July and lasted about 2 hours. A view of the fieldwork is shown in Figure 2.



Figure 2: a) fieldwork at the IT.SNZ1 seismic station. b) 2D array geometry (UTM coordinates).



The geometry of the array controls the response in terms of theoretical transfer function as described in Figure 3. On the left, the array transfer function is shown. On the right, the limits for the aliasing conditions are reported both in slowness and in velocity domains.

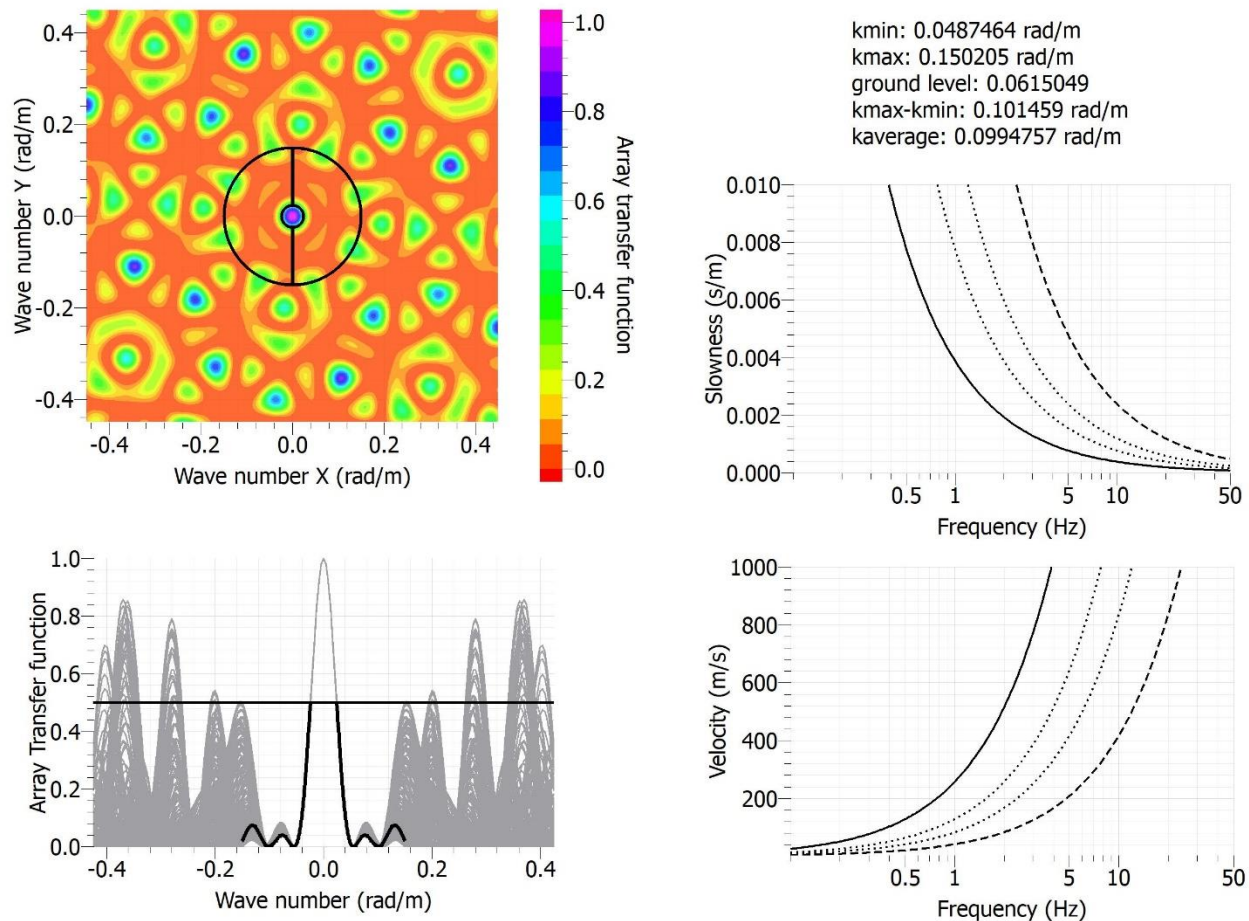


Figure 3: on the left, the theoretical array transfer function is reported for the 2D array. On the right, the aliasing conditions are reported in the slowness and velocity domains.



The H/V curves of the 9 stations are superimposed on each other in Figure 4, where the average H/V is reported in red. There is a general agreement of the H/V shapes showing a good overlapping at all the frequencies in the range 0.1-15 Hz. The resonance frequency (f_0) is assigned at 0.7 Hz ($\sigma = 0.12$ Hz). The rotated HV spectral ratios do not show any significant polarization effect (Figure 5).

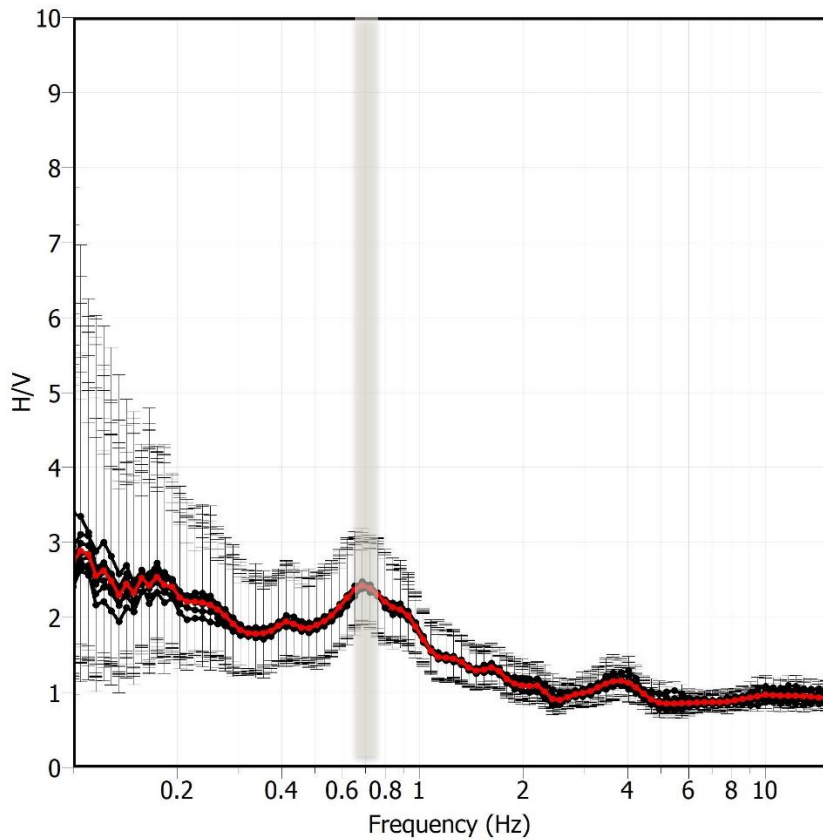


Figure 4: H/V curves of the 9 stations of the 2D array. The average is reported in red. The vertical bars estimate the H/V uncertainties.

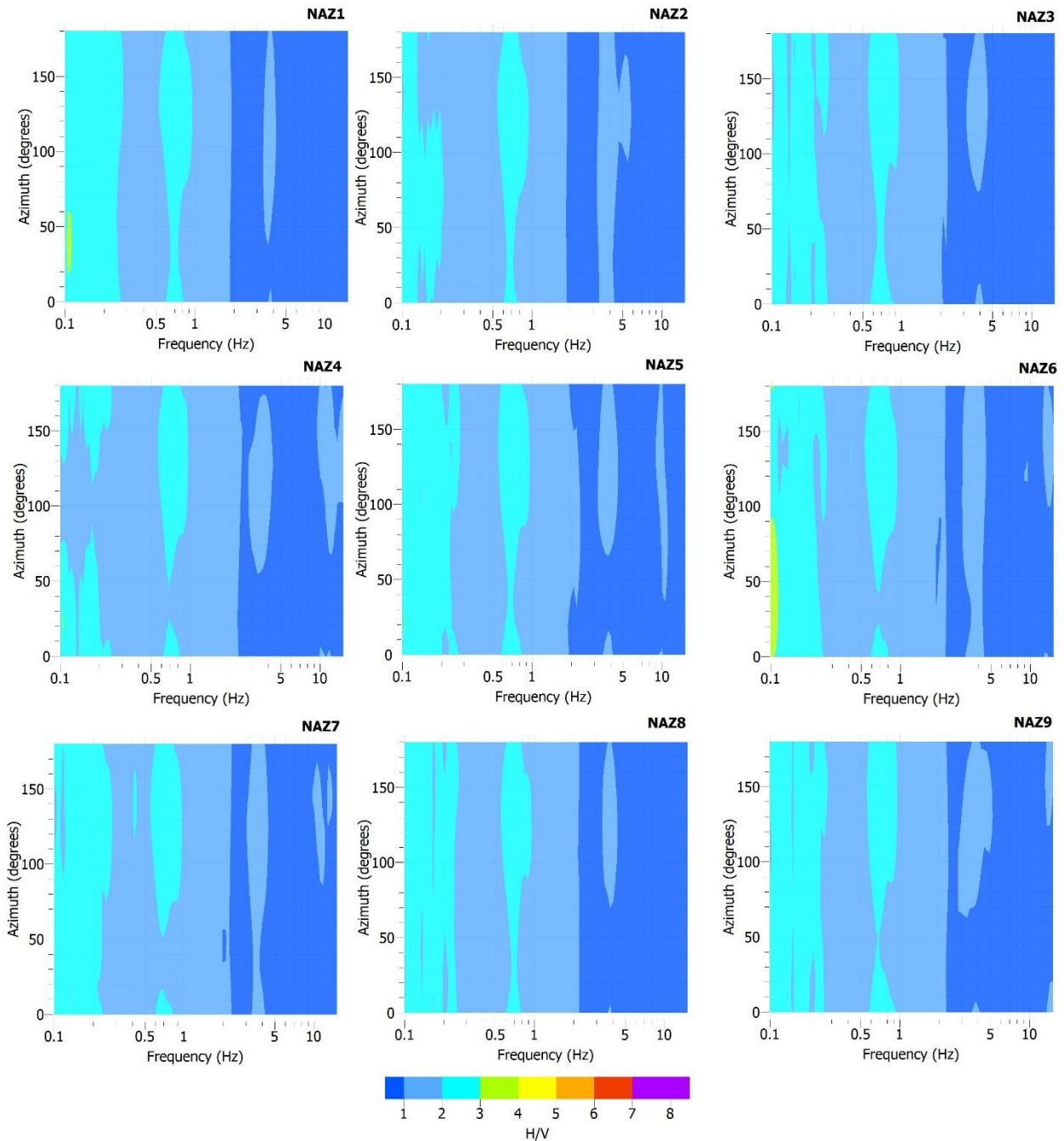


Figure 5: rotated H/V curves for the 9 stations of the 2D array.



Data from the 2D array have been analyzed with the GEOPSY code (<http://www.geopsy.org>) in terms of high-resolution FK analysis. The dispersion curve obtained from the vertical components is shown in Figure 6, whereas the dispersion curve obtained from the horizontal components is shown in Figure 7. We interpret and assume that the dispersion curve obtained in Figure 6 is relative to the fundamental mode of the Rayleigh dispersive waves. On the other hand, we interpret that the dispersion curve obtained in Figure 7 is relative to the fundamental mode of the Love dispersive waves. The aliasing conditions (black lines) constrain the validity range of the picked dispersion curves in the frequency range 2-5 Hz.

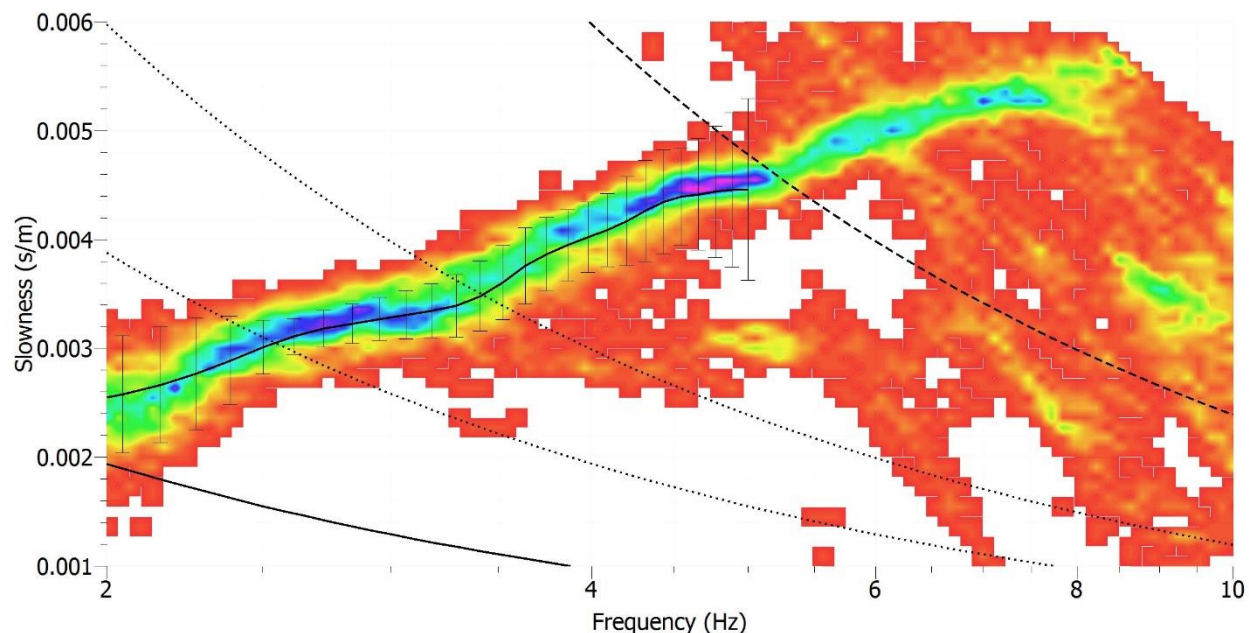


Figure 6: Picked dispersion curve in the slowness domain with the high-resolution FK analysis on the vertical components. The limits for the aliasing conditions are reported with black lines.

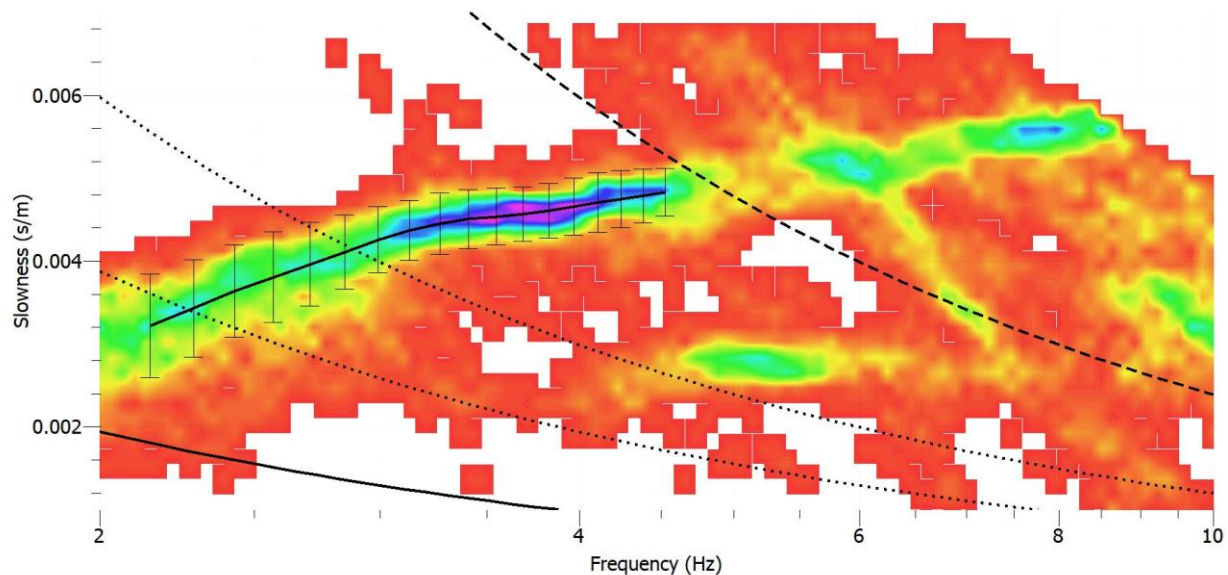
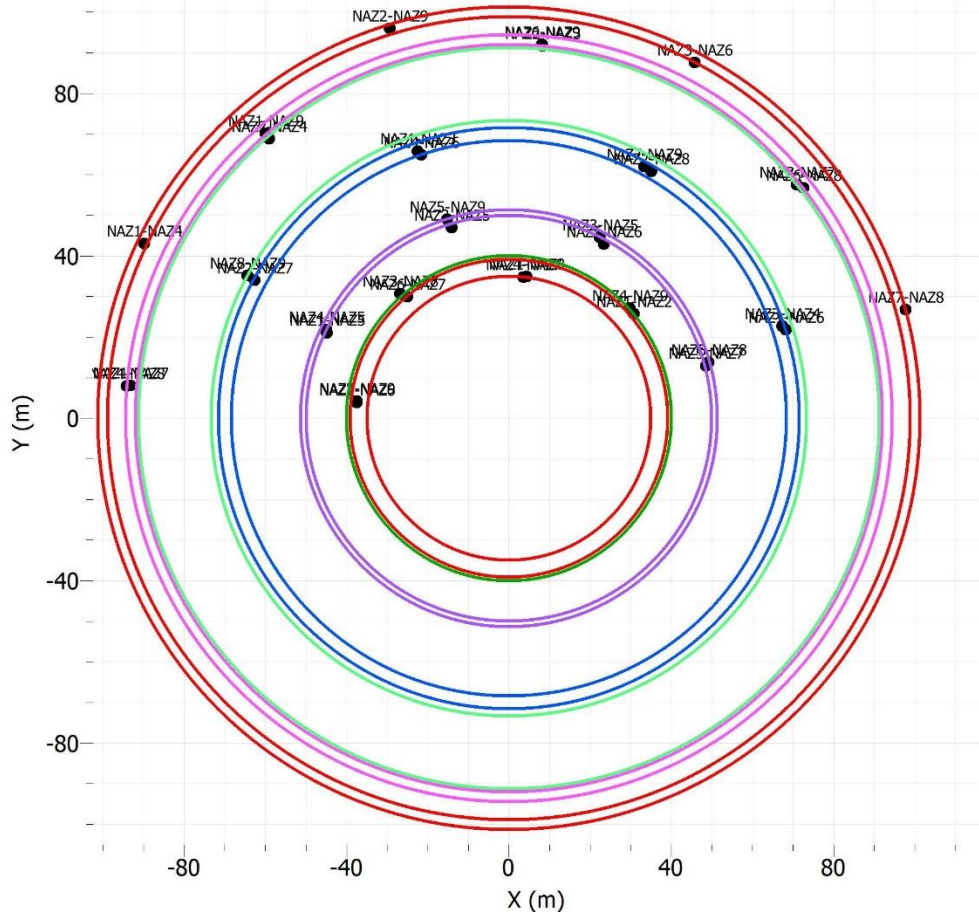


Figure 7: Picked dispersion curve in the slowness domain with the high-resolution FK analysis on the transverse components. The limits for the aliasing conditions are reported with black lines.

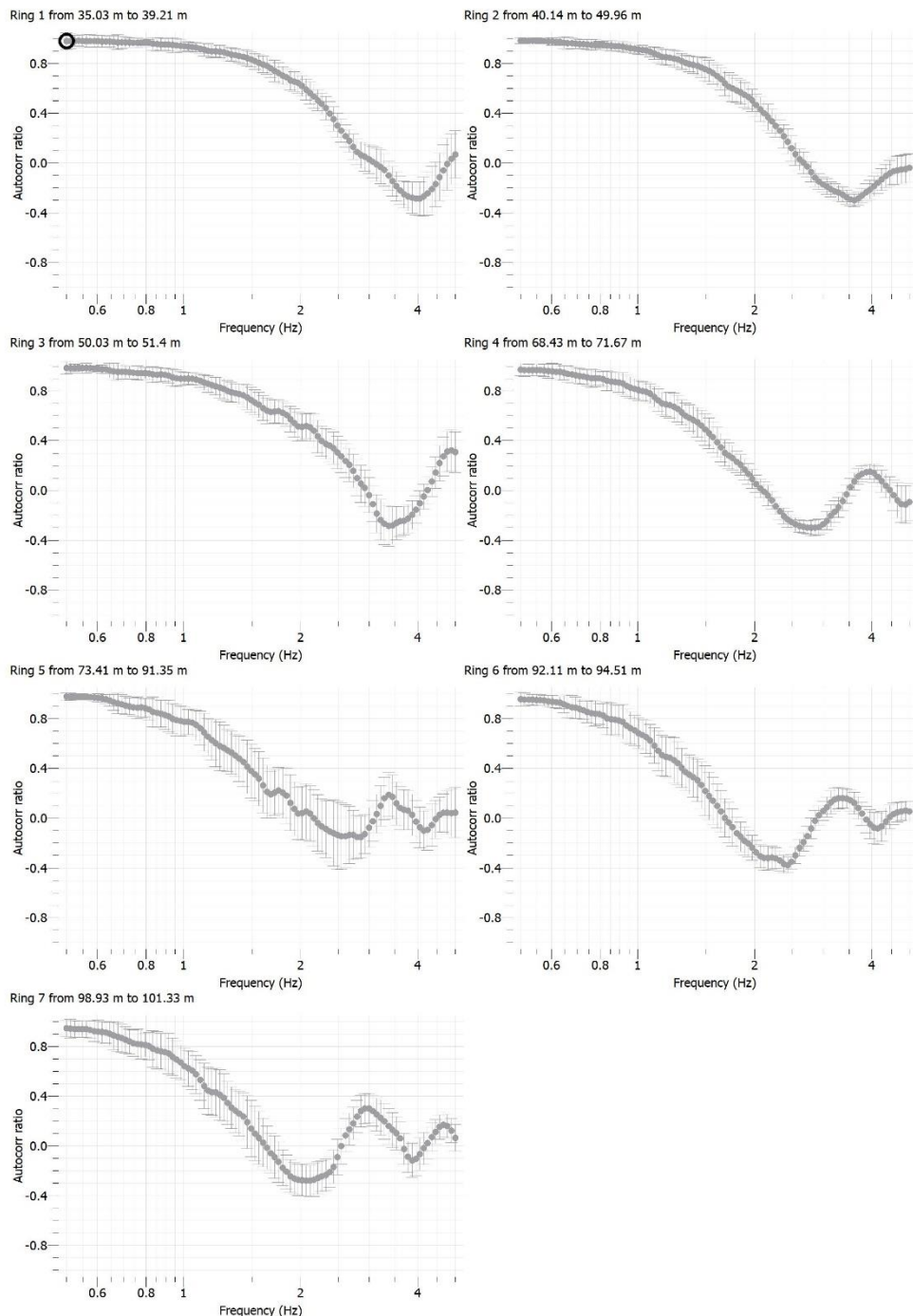
The modified spatial autocorrelation technique (MSPAC) has also been applied to the passive data to obtain the autocorrelation curves. Figure 8a shows the 7 rings adopted for the MSPAC analysis, whose geometries are reported in Table 2. Figure 8b shows the spatial autocorrelation curves computed for each ring.

Ring	R min [m]	R max [m]	Pairs
1	35.03	39.21	5
2	40.14	49.96	7
3	50.03	51.4	4
4	68.43	71.67	7
5	73.41	91.35	3
6	92.11	94.51	6
7	98.93	101.33	4

Table 2: geometry of the 7 rings adopted for the MSPAC analysis.



a)



b)

Figure 8: a) rings selected for the MSPAC analysis; b) autocorrelation curves of the 7 rings.



The auto-correlation curves in Figure 8b have been inverted to obtain the corresponding dispersion curve (Figure 9) that we assume as relative to the fundamental mode of the Rayleigh dispersive waves in the frequency range 0.6-3 Hz.

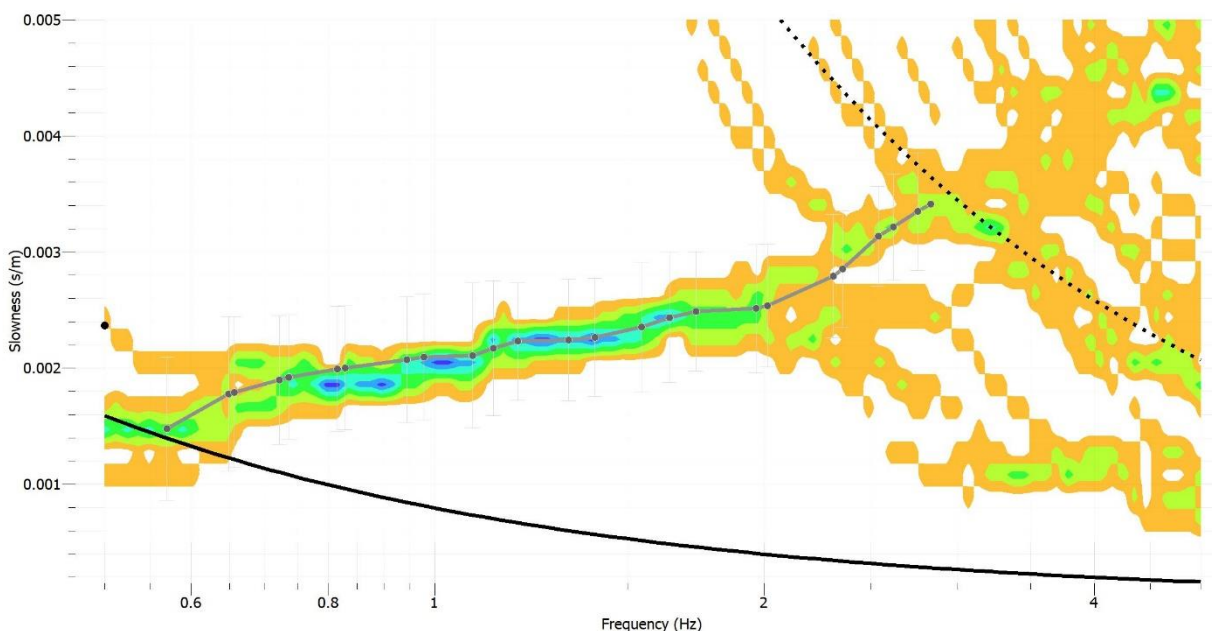
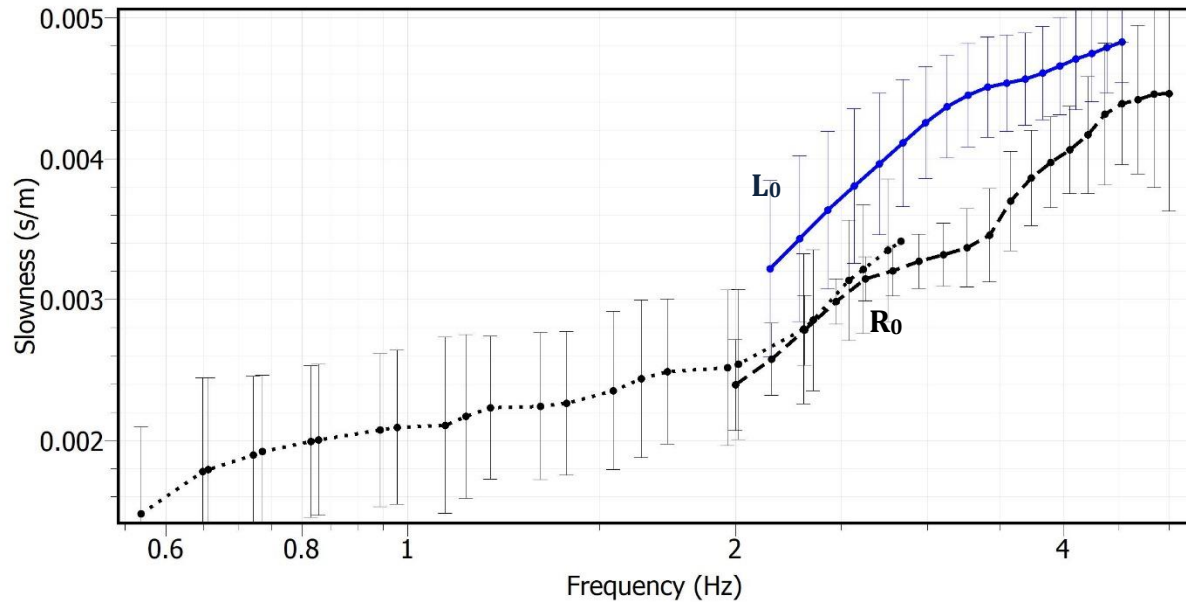


Figure 9: picked dispersion curve in the slowness domain with the MSPAC method.

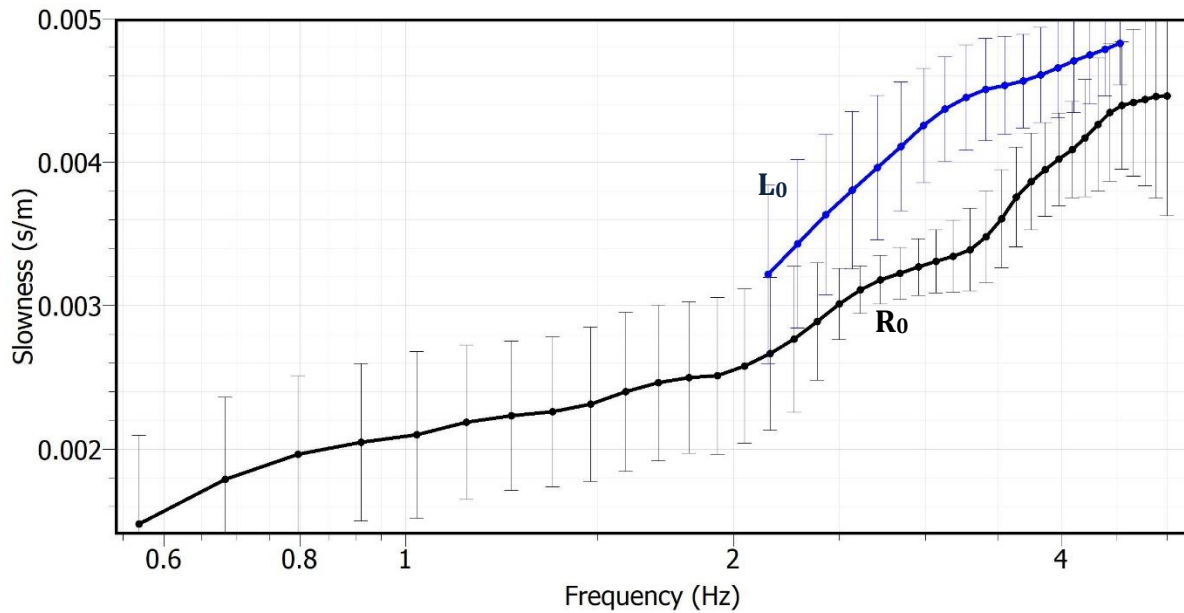
3. SEISMIC VELOCITY MODEL

Comparing the dispersion curves obtained from the FK and MSPAC analyzes, we observe a good consistency. In particular, the FK dispersion curve extends to higher frequency (2-5 Hz), whereas the MSPAC dispersion curve extends to lower frequency (0.6-3 Hz).

The FK and MSPAC dispersion curves are superimposed in Figure 10a and the final dispersion curves, adopted for the inversion process, is shown in Figure 10b.



a)



b)

Figure 10: a) Superimposed FK and MSPAC dispersion curves in their validity limits. In black the dispersion curves relative to the fundamental mode of the Rayleigh waves, obtained from both the MSPAC (dotted) and the FK (dashed)



methods. In blue the dispersion curve relative to the fundamental mode of the Love waves. b) Dispersion curves adopted for the inversion process. R0: fundamental mode of Rayleigh waves; L0: fundamental mode of Love waves.

To proceed with the inversion, we estimate the ellipticity curve from the H/V curve, considering in particular the right flank of the H/V peak that carries the important information on the underground structure. However, to reproduce the H/V peak we consider also the left flank. To reduce the contribution of the other waves in the H/V flanks, a common practice consists in reducing the H/V amplitude for the square root of 2 (Foti et al., 2011). The estimated ellipticity curve is reported in Figure 11 (blue curves) together with the average H/V curve (black curve).

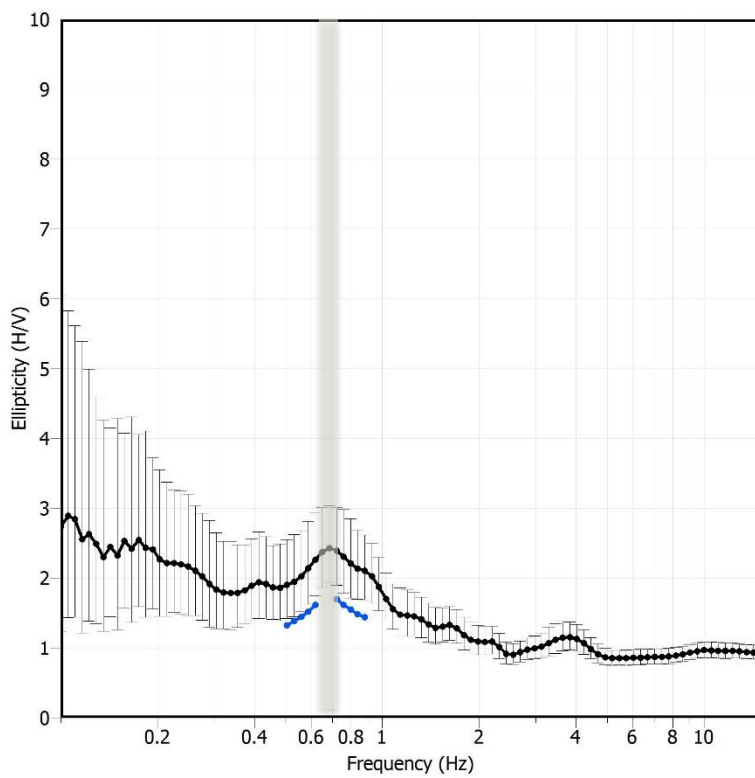


Figure 11: estimation of the ellipticity curve (blue) from the average H/V curve (black). The vertical bars estimate the H/V uncertainties.



Finally, we jointly invert the following targets:

- 1) Rayleigh wave and Love wave dispersion curves (fundamental mode) in Figure 10b;
- 2) ellipticity curve in Figure 11 (blue curves);
- 3) $f_0 = 0.7$ Hz estimated from H/V curves .

The resulting models after the inversion step are shown in Figure 12. We obtained a fairly good fit between experimental and theoretical curves using a model parameterization composed of three main layers over halfspace.

Focusing on the V_s models of Figure 12, the results indicate a first soft layer with thickness <20 m and V_s around 176 m/s. A second layer shows V_s of 318 m/s down to 46 m in depth, where a third layer is characterized by V_s values of 481 m/s. The halfspace is found at 177 m in depth with $V_s > 800$ m/s.

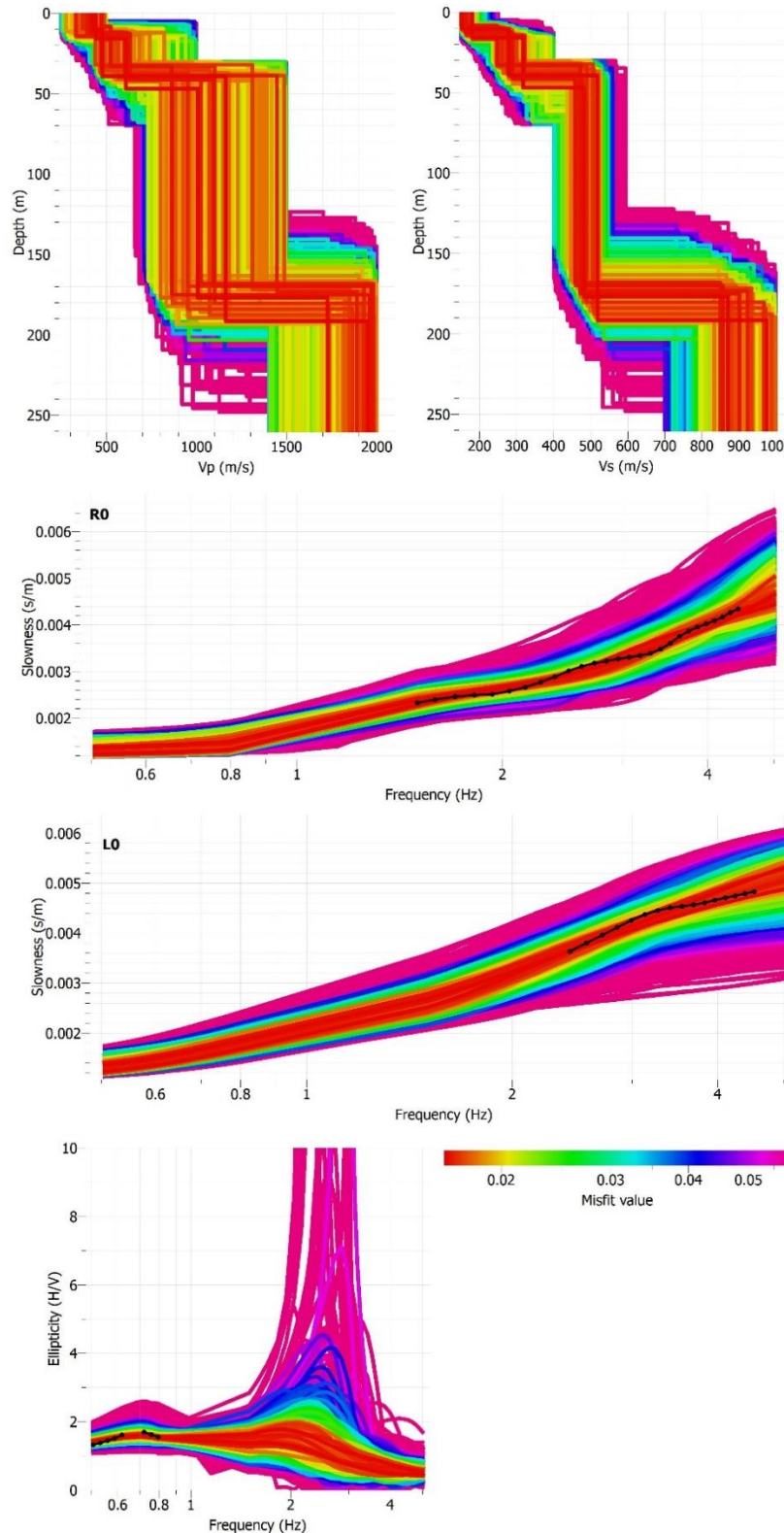




Figure 12: Inversion of the dispersion curves obtained with the 2D passive array, constrained with the H/V results (the field data are shown as black curves).

The best V_p and V_s model (i.e. lowest misfit) resulting from the inversion are proposed in Figure 13 and Table 3.

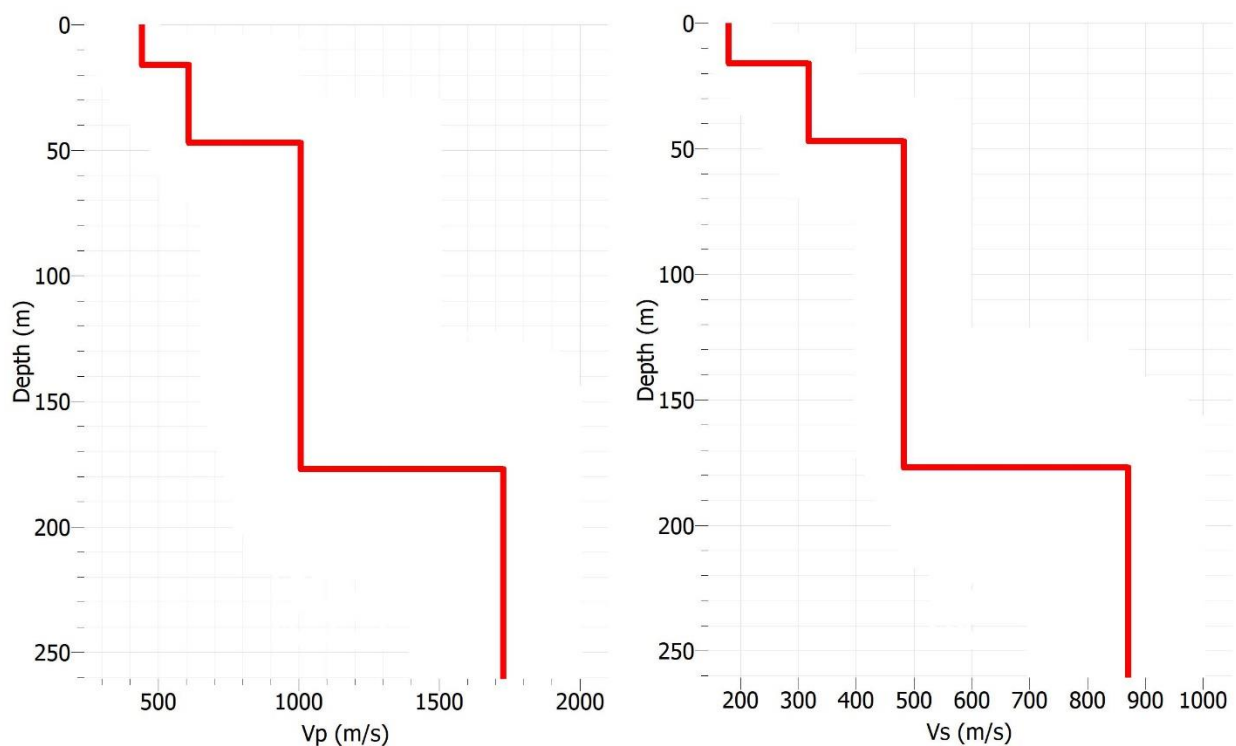


Figure 13: Best-fit models of V_p (left panel) and V_s (right panel) values.

From	To	Thickness [m]	V_s [m/s]	V_p [m/s]
0	16	16	176	435
16	46	30	318	605
46	177	131	481	1006
177	?	?	871	1722

Table 3: Best-fit model



4. CONCLUSIONS

The surface-wave analysis at the IT.SNZ1 seismic station indicates a soft site, where the resonance frequency of the soil deposits is at 0.7 Hz, suggesting a bedrock relatively deep.

To assess the Vs profile of the site, a joint inversion of the Rayleigh wave and Love wave dispersion curves (fundamental mode only) was performed, with the additional constrain of the estimated ellipticity curve. The Vs profile was subsequently correlated to the stratigraphic model provided in the geological report at IT.SNZ1 (Working group INGV (2019). Geological report at the seismic station IT.SNZ1; Figure 14).

A first layer with thickness <20 m and Vs around 176 m/s correlates to the shallow gravel and sand deposit observed on the geological section at the IT.SNZ1 site (Figure 14). A deeper layer shows Vs of 318 m/s down to 46 m in depth, in correspondence to a stratigraphic layer characterized by alternations of clay, sand and silt. At greater depth, Vs values of 481 m/s are observed in correspondence to sand and gravels with lens of silt and clay (Figure 14). The halfspace, constrained with the ellipticity curve at 0.7 Hz, is found at 177 m in depth with Vs > 800 m/s.

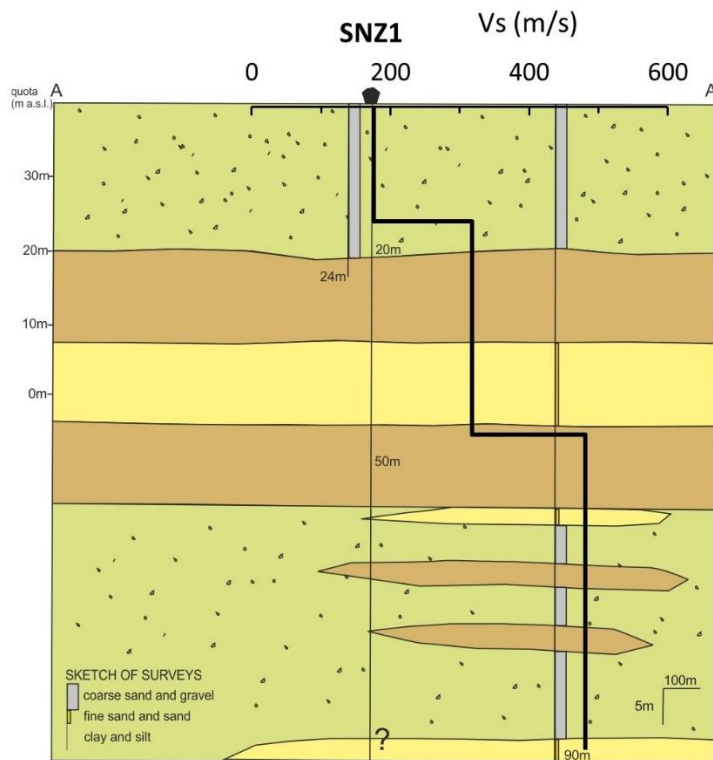


Figure 14: correlation between geological and geophysical information at the IT.SNZ1 site (geological section from Working group INGV (2019). Geological report at the seismic station IT.SNZ1 – San Nazzaro).

According to the current Italian seismic code (NTC 2018), if the bedrock ($V_s > 800 \text{ m/s}$) is more than 30 m in depth, the equivalent velocity ($V_{s,eq}$) is equal to the $V_{s,30}$. This is the case of the IT.SNZ1 site, where the $V_{s,30}$ computed from the available V_s profile is 222 m/s, and the site is classified in the soil category C for both the NTC18 and EC8 seismic classifications (Table 4).

$V_{s,eq} = V_{s,30}$ [m/s]	Soil class (NTC 2018)	Soil class (EC8)
222	C	C

Table 4: Soil Class



REFERENCES

EC8: European Committee for Standardization (2004). Eurocode 8: design of structures for earthquake resistance. P1: General rules, seismic actions and rules for buildings. Draft 6, Doc CEN/TC250/SC8/N335.

Foti, S., S. Parolai, D. Albarello, and M. Picozzi (2011). Application of surface-wave methods for seismic site characterization, *Surv. Geophys.* 32, no. 6, 777–825.

NTC 2018: Ministero delle Infrastrutture e dei Trasporti (2018). Aggiornamento delle Norme Tecniche per le Costruzioni. Part 3.2.2: Categorie di sottosuolo e condizioni topografiche, Gazzetta Ufficiale n. 42 del 20 febbraio 2018 (in Italian).

Working group INGV "Agreement DPC-INGV 2019-21. All.B2 – WP1, Task 2", (2019). Geological report at the seismic station IT. SNZ1 – Milano. <http://hdl.handle.net/2122/12936>



Disclaimer and limits of use of information

The INGV, in accordance with the Article 2 of Decree Law 381/1999, carries out seismic and volcanic monitoring of the Italian national territory, providing for the organization of integrated national seismic network and the coordination of local and regional seismic networks as described in the agreement with the Department of Civil Protection.

INGV contributes, within the limits of its skills, to the evaluation of seismic and volcanic hazard in the Country, according to the mode agreed in the ten-year program between INGV and DPC February 2, 2012 (Prot. INGV 2052 of 27/2/2012), and to the activities planned as part of the National Civil Protection System.

In particular, this document¹ has informative purposes concerning the observations and the data collected from the monitoring and observational networks managed by INGV.

INGV provides scientific information using the best scientific knowledge available at the time of the drafting of the documents produced; however, due to the complexity of natural phenomena in question, nothing can be blamed to INGV about the possible incompleteness and uncertainty of the reported data.

INGV is not responsible for any use, even partial, of the contents of this document by third parties and any damage caused to third parties resulting from its use.

The data contained in this document is the property of the INGV.



This document is licensed under License

Attribution – No derivatives 4.0 International (CC BY-ND 4.0)

¹This document is level 3 as defined in the "Principi della politica dei dati dell'INGV (D.P. n. 200 del 26.04.2016)"



Esclusione di responsabilità e limiti di uso delle informazioni

L'INGV, in ottemperanza a quanto disposto dall'Art.2 del D.L. 381/1999, svolge funzioni di sorveglianza sismica e vulcanica del territorio nazionale, provvedendo all'organizzazione della rete sismica nazionale integrata e al coordinamento delle reti sismiche regionali e locali in regime di convenzione con il Dipartimento della Protezione Civile.

L'INGV concorre, nei limiti delle proprie competenze inerenti la valutazione della Pericolosità sismica e vulcanica nel territorio nazionale e secondo le modalità concordate dall'Accordo di programma decennale stipulato tra lo stesso INGV e il DPC in data 2 febbraio 2012 (Prot. INGV 2052 del 27/2/2012), alle attività previste nell'ambito del Sistema Nazionale di Protezione Civile.

In particolare, questo documento ha finalità informative circa le osservazioni e i dati acquisiti dalle Reti di monitoraggio e osservative gestite dall'INGV.

L'INGV fornisce informazioni scientifiche utilizzando le migliori conoscenze scientifiche disponibili al momento della stesura dei documenti prodotti; tuttavia, in conseguenza della complessità dei fenomeni naturali in oggetto, nulla può essere imputato all'INGV circa l'eventuale incompletezza ed incertezza dei dati riportati.

L'INGV non è responsabile dell'utilizzo, anche parziale, dei contenuti di questo documento da parte di terzi e di eventuali danni arrecati a terzi derivanti dal suo utilizzo.

La proprietà dei dati contenuti in questo documento è dell'INGV.



Quest'opera è distribuita con Licenza

Creative Commons Attribuzione - Non opere derivate 4.0 Internazionale.

1Questo documento rientra nella categoria di livello 3 come definita nei "Principi della politica dei dati dell'INGV (D.P. n. 200 del 26.04.2016)".